Metabolomics and network pharmacology reveal antibacterial components and mechanisms in citrus herbs

Yan Li[1,2*], Lu He[3], Yu Liang[1]

[1]*School of Food and Pharmaceutical Engineering, Zhaoqing University, Zhaoqing, Guangdong Province, PR China;* [2]*Lushan Botanical Garden, Jiangxi Province and Chinese Academy of Science, Jiujiang, Jiangxi Province, PR China;* [3]*Shenzhen Qianhai Shekou Free Trade Zone Hospital, Shenzhen, Guangdong Province, PR China*

***Corresponding Author:** Yan Li, School of Food and Pharmaceutical Engineering, Zhaoqing University, Zhaoqing, Guangdong Province, PR China; Lushan Botanical Garden, Jiangxi Province and Chinese Academy of Science, Jiujiang, Jiangxi Province, PR China. Email: yan.li99@foxmail.com

Academic Editor: Walid Elfalleh, PhD, Department of Life Sciences, Al Imam Mohamed Ibn Saud Islamic University (IMSIU), 11623 Riyadh, Saudi Arabia & Higher Institute of Applied Sciences and Technology of Gabes (ISSATGb), Tunisia

Received: 13 April 2025; Accepted: 12 September 2025; Published: 14 November 2025

RESEARCH ARTICLE

Abstract

This study evaluated the potential antibacterial activity and chemical profiles of four citrus herbs: Chenpi (CP), Qingpi (QP), Zhike (ZK), and Zhishi (ZS). The total flavonoid content was significantly higher in the QP extract compared to CP, as well as in the ZK extract compared to ZS. Additionally, the QP extract demonstrated stronger antibacterial activity than the CP extract with a minimum inhibitory concentration (MIC) of 2.5 mg/mL against both *Bacillus cereus* and methicillin-resistant *Staphylococcus aureus* (MRSA). Similarly, the ZK extract exhibited greater potency than ZS, exhibiting MICs of 1.25 mg/mL against *B. cereus* and 2.5 mg/mL against MRSA. Metabolomic analysis revealed variations in the concentration of chemical compounds among the four citrus herb extracts. Notably, (–)-quinic acid levels were significantly elevated in the QP extract compared to the CP extract. The ZK extract showed markedly higher concentrations of key flavonoids, including hesperidin, naringin, and hesperetin 7-*O*-neohesperidoside, relative to ZS. The upregulated accumulated metabolites in the QP and ZK extracts were analyzed using network pharmacology to predict their potential antibacterial targets against bacterial infections. Core targets associated with bacterial infections, including TNF, MMP2, and AKT1, were identified. These findings highlight citrus herbs, particularly QP and ZK, as promising antibacterial candidates.

Keywords: antibacterial activity; citrus herbs; metabolomics; network pharmacology

Introduction

The genus *Citrus*, belonging to the Rutaceae family, is globally recognized for its edible fruits and use as a source of pharmacological herbs. A variety of citrus species are cultivated in China, often processed into traditional Chinese medicine, for instance, the dried ripe fruit of *Citrus aurantium* L. (Zhike; ZK), the dried unripe fruit of *C. aurantium* L. (Zhishi; ZS), the dried mature pericarp of *Citrus reticulata* Blanco (Chenpi; CP), the dried immature pericarp of *C. reticulata* Blanco (Qingpi; QP), the dried mature fruit of *Citrus medica* L. (Xiangyuan; XY), the dried exocarp of immature or nearly mature *Citrus grandis* (L.) Osbeck (Huajuhong; HJH), and the dried fruit of *C. medica* L. var. sarcodactylis Swingle (Foshou; FS) (Chen *et al*., 2021; Tian *et al*., 2019). It has

 ISSN 1757-837X online, DOI 10.15586/qas.v17i4.1590

been reported that citrus varieties contain various bioactive components, including essential oils, flavonoids, limonoids, and alkaloids, which contribute to their beneficial effects on human health (D'Amore *et al*., 2024; Maqbool *et al*., 2023). Many citrus compounds exhibit potential health-promoting effects. Among these, citrus essential oils possess notable antibacterial activity against numerous bacteria (Ellouze *et al*., 2024). The essential oils of *C. aurantium* and *Citrus sinensis* have been shown to influence brain activity and produce anxiolytic effects (Mannucci *et al*., 2018). Flavonoids, such as neohesperidin and polymethoxyflavones, derived from citrus are primarily associated with antiproliferative properties, radical-scavenging effects, inhibition of microbial growth, alleviation of inflammation, and suppression of cardiovascular diseases (Akhter *et al*., 2024; Gao *et al*., 2018; Zhao *et al*., 2018). Citrus limonoids, typically found in the peels of citrus fruits, possess antibacterial, antioxidant, and anti-angiogenic properties (Liu *et al*., 2021). Additionally, the main alkaloid components in citrus herbs, synephrine and *N*-methyltyramine, have been studied for their health benefits. For example, synephrine aids in weight loss by promoting metabolism and increasing calorie expenditure (Liu *et al*., 2021; Yu *et al*., 2018). *N*-methyltyramine, a naturally occurring trace amine, has emerged as a promising candidate for modulating adrenergic receptor signaling in the treatment of gastrointestinal disorders (Ni *et al*., 2019). Thus, citrus herbs, as both food and medicinal resources, play a crucial role in the regulation and prevention of various diseases (Hao *et al*., 2024; Ma *et al*., 2022).

The citrus essential oils have demonstrated antimicrobial activity against *Escherichia coli* and *Lactobacillus acidophilus*, as well as efficacy in controlling the growth of fungi, including *Aspergillus niger* and *Penicillium expansum* (Cebi *et al*., 2023; Tang *et al*., 2023). These properties suggest their potential as antibiotic alternatives, aiding in extending the shelf life of food products. This study reveals the potential antibacterial activity of four citrus herbs, QP, CP, ZK, and ZS. Many studies have focused on citrus herbs, typically employing chromatographic separation, spectrometric analysis, and bioactivity detection (Wang *et al*., 2025; Zhou *et al*., 2022). Recently, rapid and efficient tools, such as pharmacophore analysis, network pharmacology, and molecular docking, have emerged in the field of pharmacology (Guo *et al*., 2021; S. Zhao *et al*., 2018). However, limited research has explored the antibacterial activity of citrus herbs using a combined experimental and computational approach to identify potential antibacterial small molecules and their mechanisms of action. In this study, we investigated the underlying antibacterial mechanisms of citrus herbs by integrating metabolomics analysis and network pharmacology. We identified the core targets of the potential active ingredients in citrus herbs for treating bacterial infections. Moreover, the proposed potential active components and main targets were verified using molecular docking technology. This study provides valuable insights into the possible antibacterial citrus herbs, which could be further explored for the development of complementary medicinal formulations or sanitizers to help manage bacterial infections.

Materials and Methods

Plant materials and preparation of plant extracts

Citrus herb samples, including CP, QP, ZK, and ZS, were purchased from Juyaotang Co., Ltd. (Anguo, China). For the preparation of the herb extracts, 2.5 g of powdered material was macerated in 100 mL of solvent mixture comprising methanol, acetonitrile, and water (2:2:1, v/v/v) and sonicated for 30 min. The solvent extracts were then filtered through filter paper, and the filtrates were evaporated to dryness using a rotary evaporator. The resulting dried extracts were stored at −20 °C until further use.

Determination of total phenolic content and total flavonoid content

The total phenolic content (TPC) and total flavonoid content (TFC) of the citrus herb extracts were determined. The TPC was assessed according to a previously reported method (Adusei *et al*., 2019) with some modifications. Briefly, 1 mL of appropriately diluted extract (1 mg/mL) was mixed with 0.5 mL of freshly prepared Folin–Ciocalteu reagent, 1 mL of a 7.5% sodium carbonate solution, and 7.5 mL of distilled water. The reaction mixture was incubated in the dark for 1 h at room temperature. Absorbance was measured at 765 nm against a blank, which was prepared identically but with distilled water replacing the extract. TPC was quantified against a gallic acid (GA) standard curve and expressed as milligrams of GA equivalents per gram of extract (mg GAE/g extract). The TFC was measured as described by Shraim *et al*. (2021). Briefly, 500 µL of the sample (1 mg/mL) was mixed with 0.15 mL of sodium nitrite solution, 0.15 mL of a 10% aluminum nitrate solution, 2 mL of a 4% sodium hydroxide solution, and 2.2 mL of distilled water. After incubation at room temperature for 15 min, the absorbance was measured at 508 nm. TFC was determined using a rutin calibration curve expressed as milligrams of rutin equivalents per gram of extract (mg RE/g extract). Each experiment was carried out with three replicates.

Antibacterial activity of citrus herb extracts

The *Bacillus cereus* CMCC 63302 (*B. cereus*) and *E. coli* ATCC 8739 (*E. coli*) strains were purchased from Guangdong Microbial Culture Collection Center (Guangzhou, China). Methicillin-resistant *S. aureus* 4469 (MRSA) was generously provided by Dr. Bailin Li at the South China Botanical Garden. Prior to the experiment, the bacterial strains were cultured in nutrient broth for 24 h at 37 °C with shaking. The bacterial suspension was then adjusted to a final inoculum density of 1–5 × 10^5 cfu/mL based on its optical density at 600 nm (Li *et al*., 2023).

All extracts of citrus herbs were dissolved in dimethyl sulfoxide (DMSO) and diluted with sterilized water to obtain a 10% aqueous DMSO solution. The antibacterial activity of the samples was measured in sterile 96-well plates. Each well received 100 μL of sample extract (at concentrations of 5, 2.5, 1.25, 0.63, 0.31, and 0.16 mg/mL) and 100 μL of the bacterial suspension. Control wells contained 100 μL of bacterial suspension with either 100 μL of 25 μM ampicillin (positive control) or 100 μL of 10% aqueous DMSO (blank) in place of the citrus herb extract. The microbial growth inhibition curve was recorded every 2 h by measuring the absorbance at 600 nm over a period of 16 h. For each sample, all assays were conducted in triplicate.

Metabolome analysis of citrus herbs using LC-MS/MS

Citrus herb samples (25 mg) were extracted with 1000 μL of solvent mixture composed of methanol, acetonitrile, and water in the ratio 2:2:1 (v/v/v) containing deuterated internal standards. The mixed solution was vortexed for 30 s, homogenized for 4 min, and sonicated for 5 min in an ice-water bath at 4 °C. This vortex–homogenization–sonication cycle was repeated twice more for a total of three cycles. The samples were subsequently incubated under −40 °C for 1 h to precipitate proteins. Following incubation, the samples were centrifuged at 12,000 rpm at 4 °C for 15 min. The supernatant was collected and centrifuged again under identical conditions. The resulting supernatant was filtered through a 0.22 μm microporous membrane. A quality control (QC) sample was prepared by pooling equal volumes of the final supernatant from each individual citrus herb sample.

To obtain the metabolomic profile of citrus herbs, LC-MS/MS analysis was performed using an UHPLC system (Vanquish, Thermo Fisher Scientific) equipped with a Phenomenex Kinetex C18 column (2.1 mm × 50 mm, 2.6 μm) coupled to an Orbitrap Exploris 120 mass spectrometer (Orbitrap MS, Thermo). Mobile phase A consisted of 0.01% acetic acid in water, and mobile phase B was a mixture of isopropanol and ACN (1:1, v/v). The column temperature was maintained at 25 °C, and the autosampler temperature was set to 4 °C, with an injection volume of 2 μL. The total separation time was 6 min. The MS/MS spectra were acquired in information-dependent acquisition (IDA) mode, controlled by the acquisition software (Xcalibur, Thermo). In this mode, the acquisition software continuously evaluated the full scan MS spectrum. The electrospray ionization (ESI) source conditions were optimized based on the reported method (Chen *et al*., 2022) and set as follows: sheath gas flow rate at 50 Arb; aux gas flow rate at 15 Arb; capillary temperature at 320 °C; sweep gas at 1 Arb; vaporizer temperature at 350 °C; full MS resolution at 60,000; MS/MS resolution at 15,000; collision energy at 20/30/40 SNCE; and spray voltage at 3.8 kV (positive) or −3.4 kV (negative), respectively. All citrus herb extracts were analyzed in triplicate.

Network construction

To identify the potential active ingredients in citrus herbs, all upregulated differentially accumulated metabolites (DAMs) were subjected to the Traditional Chinese Medicine Systems Pharmacology Database and Analysis Platform (TCMSP) based on the following drug screening criteria: Oral bioavailability (OB) ≥ 20% and Drug-likeness (DL) ≥ 0.1 (Cao *et al*., 2023). The potential active ingredients identified were then analyzed using PubChem and Swiss Target Prediction to predict associated target genes (Probability > 0.1). Concurrently, the term "bacterial infection" was employed as a keyword to retrieve bacterial-related genes from the OMIM and GeneCards databases. After compiling all targets and removing duplicates, a Venn diagram was constructed to identify the common targets between the ingredient-predicted targets and the disease-related targets. These common targets were uploaded to the STRING database, and the corresponding species were selected. Subsequently, the protein–protein interaction (PPI) network files were generated and imported into Cytoscape 3.10.3 software to screen for the core targets associated with antibacterial effects (Shady *et al*., 2024). To elucidate the functions and metabolic pathways of these core genes, they were subjected to Gene Ontology (GO) and Kyoto Encyclopedia of Genes and Genomes (KEGG) pathway enrichment analyses using the DAVID database. Finally, the results of GO and KEGG analyses were further visualized and using the bioinformatics website (https://www.bioinformatics.com.cn/).

Component–target molecular docking

Molecular docking was used to validate the interactions between small molecule ligands and core targets

identified in the network analysis. It also predicted the binding sites of small molecule ligands with their targets and assess the binding affinity (Agu *et al*., 2023). Molecular docking analysis was carried out following the approach described by Liu *et al.* (2021). In brief, the three-dimensional (3D) structure of the core target was retrieved from the Protein Data Bank (PDB) database. Using AutoDock tools 1.5.7 software, water and organic molecules were removed, nonpolar hydrogen was added, and the structure then was saved in PDBQT format. The two-dimensional (2D) structures of the active components were obtained from the PubChem database. The 2D structure was processed and transformed into PDB format through Chem3D software, and they were saved in PDBQT format as docking ligands using AutoDock Tools. The core targets served as receptors, while the active compounds were employed as ligands. The active site of molecular docking was determined by the ligand coordinate in the target protein complex. The docking process of small molecules with core targets by combining AutoDock tools with Vina. The conformation with the lowest binding affinity was selected for visualization using Pymol 2.6.2.

Statistical analysis

Antibacterial activity data, obtained from triplicate measurements, are presented as mean ± SD and were processed using Microsoft Excel 2021. For metabolomics data, statistical analysis was performed using R Studio, with $P < 0.05$ considered statistically significant.

Results and Discussion

Determination of total phenolic content and total flavonoid content

The content of phenolics and flavonoids in citrus herb extracts ranged from 1.99 mg/g to 14.79 mg/g (Figure 1). Lower TPC values were observed in the CP extract (1.99 ± 0.26 mg/g) in comparison with the results of the QP extract (2.60 ± 0.26 mg/g). The TPC in the ZK extract was measured at 2.43 ± 0.32 mg/g. Conversely, a significantly higher TPC value was recorded in the ZS extract, at 3.61 ± 0.34 mg/g. In addition, the lowest TFC of 6.42 ± 0.43 mg/g was monitored in the CP extract. In contrast, the QP extract exhibited a significantly higher TFC of 8.34 ± 0.57 mg/g. The TFC in the ZK extract was found to be almost two-fold higher (14.79 ± 0.54 mg/g) than that in the ZS extract (7.01 ± 0.46 mg/g). Therefore, there were differences observed in TPC and TFC among the four citrus herb extracts. It was reported that the flavonoid extract from pummelo peel (*Citrus maxima* (Burm.) Merr. cv. Shatian Yu) showed antibacterial activity against *Pseudomonas aeruginosa* and *S. aureus* (Liu *et al*., 2017). Several citrus flavonoids, such as naringenin, hesperidin, apigenin, rutin, quercetin, nobiletin, and tangeretin, have been documented for their potent antibacterial and frequently antifungal properties (Ciriminna *et al*., 2025). Our results suggest that the antibacterial properties of citrus herb extracts may be associated with their phenolic and flavonoid content.

Antibacterial activity of citrus herb extracts

The antibacterial efficacy of the citrus herb extracts was evaluated based on their capacity to inhibit bacterial growth. As illustrated in Figure 2, the QP extract showed an inhibitory effect on *B. cereus* with a minimum inhibitory concentration (MIC) of 2.5 mg/mL (Figure 2A). Additionally, QP extract also inhibited the growth of MRSA exhibiting an MIC of 2.5 mg/mL (Figure 2B). In contrast, CP extract did not exhibit inhibitory activity against either *B. cereus* or MRSA at the highest concentration tested (5 mg/mL). A concentration of 1.25 mg/mL of ZK extract significantly inhibited *B. cereus* (Figure 2C), while 2.5 mg/mL of ZK extract inhibited the growth of MRSA (Figure 2D). The MIC of ZS extract against *B. cereus* was 5 mg/mL, with no effect observed on MRSA. It should be noted that the highest concentration of citrus herb extracts (5 mg/mL) did not exhibit inhibitory effect on the growth of *E. coli*. Therefore, the QP extract demonstrated a more significant inhibitory effect on bacteria compared to CP extract. Similarly, ZK extract exhibited greater bacterial inhibitory ability than the ZS extract. Previous studies have reported that the citrus peel extracts exhibit broad-spectrum antibacterial effects against *E. coli*, *S. aureus*, and *Bacillus subtilis* (Zhang *et al*., 2022). Notably, the essential oil fraction of citrus peel has shown particularly effective growth inhibition against *E. coli* (Ellouze *et al*., 2024). Our extract showed no such effect against the gram-negative strain. This is likely due to the intrinsic resistance often exhibited by gram-negative strains, which possess a complex outer membrane that limits the penetration of antimicrobial compounds (Impey *et al*., 2020). Alternatively, the extraction method may have yielded the active components at a concentration below the MIC for *E. coli*. Additionally, citrus flavonoids, including nobiletin, hesperidin, and naringin, have demonstrated inhibitory effects against *Penicillium digitatum* (Costa *et al*., 2019). Based on these findings, we hypothesize that the antibacterial activity of citrus herb extracts may be attributed to naturally occurring flavonoids and essential oils.

Metabolomic profiling of citrus herbs

To correlate antibacterial activity with chemical composition, the citrus herb extracts were analyzed by LC-MS/

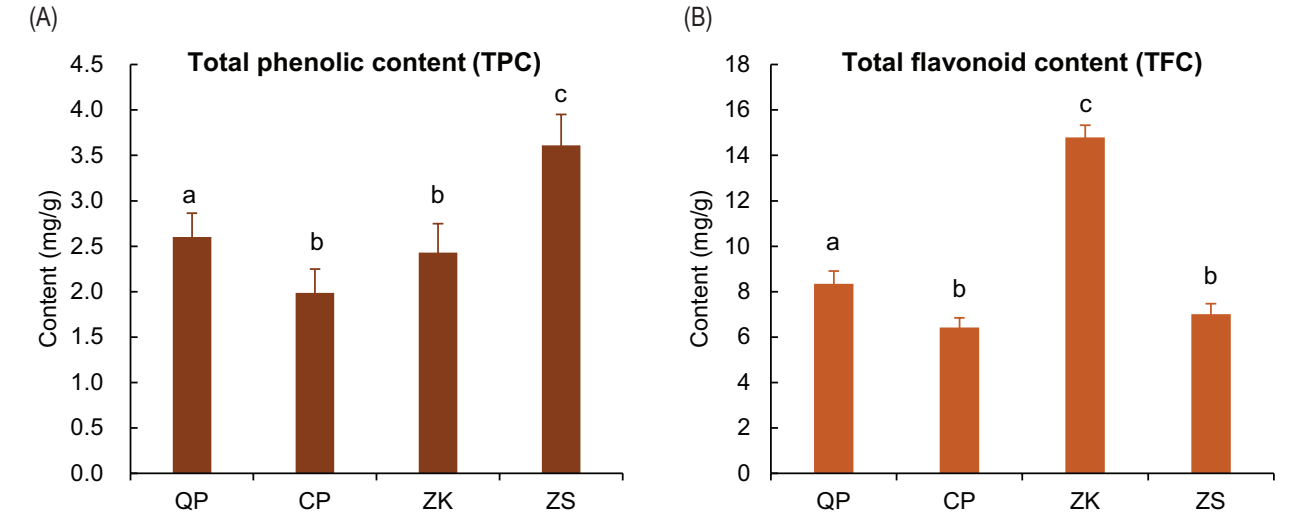

Figure 1. Total phenolic content (A) and total flavonoid content (B) in citrus herb extracts QP, CP, ZK, and ZS. Different letters above the bars represent statistically significant differences ($P < 0.05$).

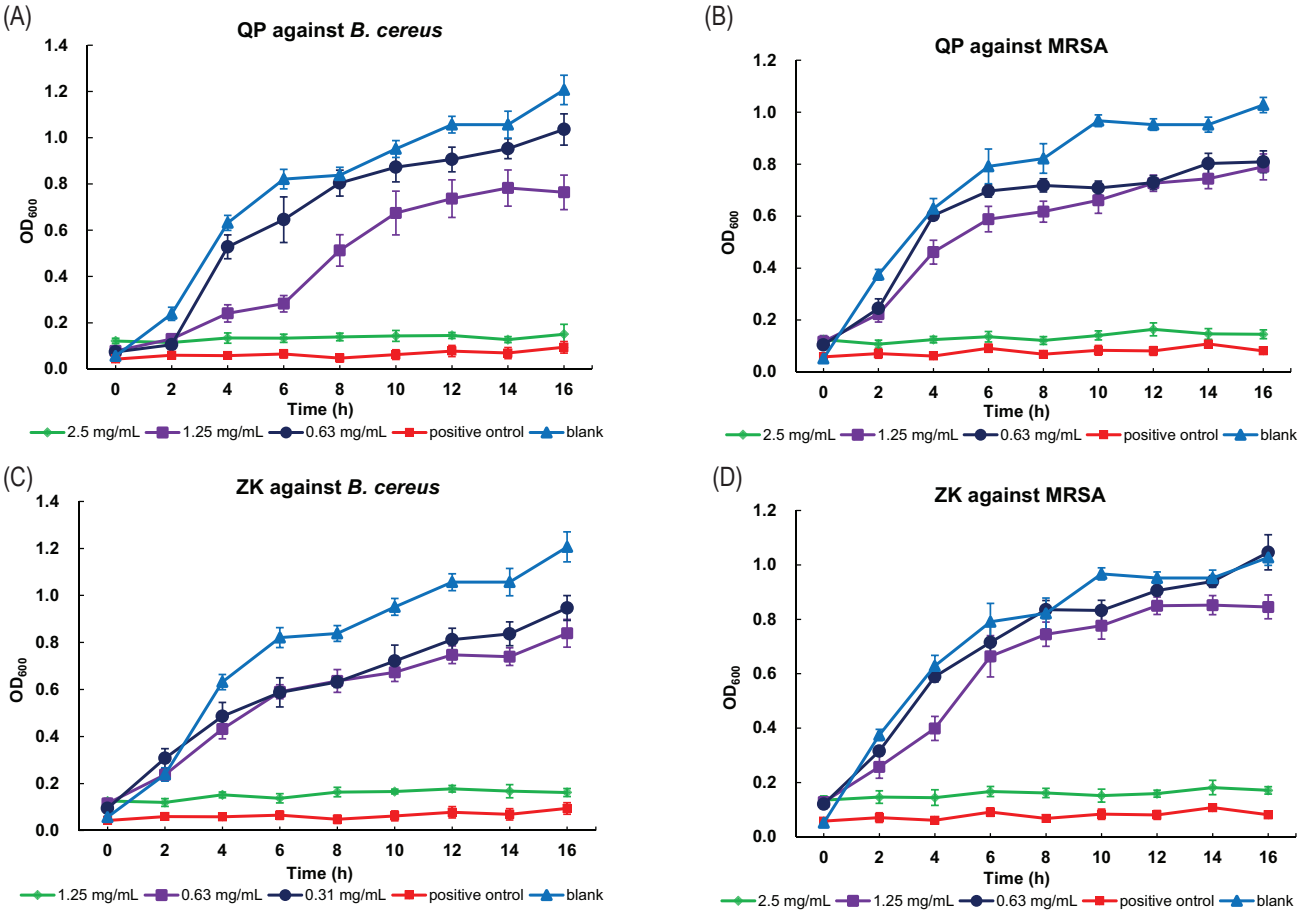

Figure 2. Bacterial inhibition experiments on citrus herb extracts. The inhibition curves of the QP extract on *B. cereus* (A) and MRSA (B) were observed over a 16-hour growth period, as well as the effects of the ZK extract on *B. cereus* (C) and MRSA (D) during the same duration. The average and standard deviation of the data were calculated based on three independent trials.

MS-based metabolomics. A total of 1009 metabolites were identified in the citrus herb extracts, including flavonoids (16.75%), fatty acids and derivatives (16.75%), terpenoids (11.99%), shikimates and phenylpropanoids (9.81%), alkaloids (8.92%), amino acids and derivatives (7.33%), phenolic acids (5.45%), polyketides (5.35%), carbohydrates (5.05%), coumarins (5.05%), and others (6.94%) (Figure 3A; Table S1). The metabolite profiles

of the citrus herbs were visualized using an orthogonal partial least squares discriminant analysis (OPLS-DA) score plot (Figure 3B). The high clustering of QC samples on the OPLS-DA score plot confirmed the stability and reliability of the chromatography and quality detection system. The four citrus herb samples were distinctly separated from one another in the score plot, particularly QP and CP, indicating significant differences in their metabolite profiles. It is essential to note that, despite the stringent QC measures and stable system performance,

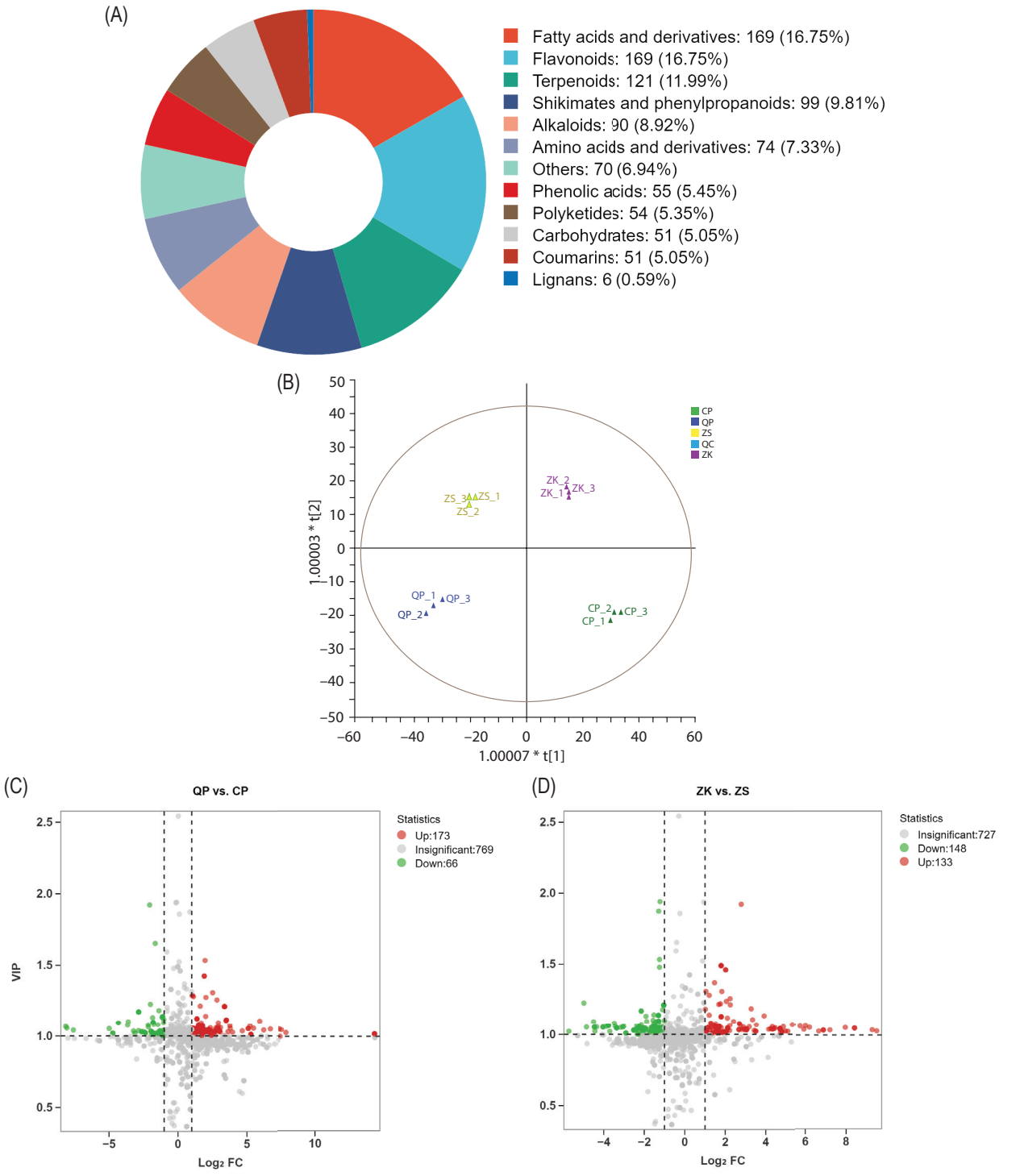

Figure 3. Metabolomic profiling reveals distinct compositional differences among citrus herb extracts. (A) Classification and proportional distribution of detected metabolites in the QP, CP, ZK, and ZS extracts. (B) The OPLS-DA plot demonstrating clear metabolic separation among QP, CP, ZK, and ZS extracts. (C) The volcano plot of differential metabolites between QP and CP extracts. Points represent individual metabolites (red: up-regulated in QP; green: down-regulated; gray: insignificant). (D) The volcano plot comparing the ZK and ZS extracts.

the untargeted LC-MS/MS approach still carries an inherent risk of false identifications due to factors such as spectral similarities, isotopic interference, and limitations in reference spectral libraries.

Variable importance in projection (VIP > 1) from OPLS-DA and fold change (FC ≥ 2 or ≤ 0.5) were utilized to identify the metabolites contributing to the differences among the citrus samples. A total of 239 differentially accumulated metabolites (DAMs) were identified as the major metabolites responsible for the variations between the QP and CP comparison groups, which included 66 downregulated and 173 upregulated DAMs (Figure 3C). Given that QP exhibited stronger antibacterial activity, the upregulated DAMs with higher concentrations in the QP extract are likely responsible for the enhanced effect. Based on this, the relative abundances of these metabolites were compared among the extracts. (–)-Quinic acid showed the highest level in both CP and QP samples, with a concentration nearly 4.6 times greater in the QP extract compared to the CP extract. Furthermore, 2-furoic acid, umbelliferone, 6-hydroxycoumarin, 7-hydroxy-4H-chromen-4-one, and aminohippuric acid were present at significantly higher concentrations in the QP sample.

A total of 281 DAMs were identified in the comparison group of ZK and ZS, comprising 133 up-regulated and 148 downregulated DAMs. The ZK sample exhibited remarkable antibacterial activity, which may be attributed to the predominant upregulated metabolites (Figure 3D). (–)-Quinic acid was also the most abundant metabolite in both ZK and ZS samples; however, its concentration did not differ significantly between the groups, with only a 1.7-fold increase in the ZK extract compared to the ZS extract. Quinic acid exhibited prominent antibacterial activity against *S. aureus* by damaging the cell membrane and disrupting cellular metabolic activity (Bai *et al*., 2022). Previous studies have reported that flavonoids are abundant in the ZK and ZS extracts, which are known to have various bioactive functions, including anti-inflammatory, antioxidant, and antibacterial activities (Zhao *et al*., 2018). In our study, the major citrus flavonoids identified were hesperidin, naringin, and hesperetin 7-*O*-neohesperidoside. The levels of these flavonoids in the ZK sample were approximately 3.5–4.2 times higher than those in the ZS sample.

Network pharmacology-based analysis

By cross-referencing the upregulated DAMs with the TCMSP database, we identified 19 potential active ingredients in the QP versus CP comparison group and 18 in the ZK versus ZS comparison group (Table S2). After searching for the target genes of these potential active ingredients and removing duplicates, we found 443 corresponding targets of potential active ingredients in the QP versus CP comparison group and 405 in the ZK versus ZS comparison group. Additionally, we selected a total of 1752 targets related to bacterial infection from the OMIM and GeneCards databases (Table S3). Notably, Venn analysis revealed 150 common targets shared between the QP vs CP comparison group and bacterial infection, as well as 140 common targets shared between the ZK versus ZS comparison group and bacterial infection (Figures 4A and 5A, Table S4). To further elucidate the role of citrus herbs in combating bacterial infection, the common targets of citrus herbs related to bacterial infection were used to construct a PPI network. Ultimately, we obtained 30 core targets concerning bacterial infection in the QP versus CP comparison group, including TNF, GAPDH, AKT1, EGFR, JUN, HIF1A, SRC, ESR1, HSP90AA1, IL2, CDK2, ERBB2, MMP9, PPARG, PTGS2, GSK3B, CXCL8, CXCR4, CCND1, MAPK1, MTOR, MMP2, APP, CTSB, JAK2, MDM2, ACE, SYK, MAPK14, and KDR (Figure 4B, Table S5). Similarly, 33 core targets associated with bacterial infection was identified in the ZK vs ZS comparison group, including TNF, GAPDH, AKT1, EGFR, HIF1A, HSP90AA1, CASP3, SRC, CDK2, ESR1, MMP9, IL2, GSK3B, PTGS2, CXCL8, MAPK1, CCND1, CXCR4, MTOR, MAPK14, CASP1, CTSB, MDM2, MAPK8, JAK2, MMP2, PARP1, APP, SYK, ABL1, SERPINE1, KIT, and EP300 (Figure 5B, Table S5). Systematic analysis of the PPI network revealed that the potential active components, including skimmin, linarin, kaempferol 3-methyl ether, limonin, 2'-*O*-methylisoliquiritigenin, bisdemethoxycurcumin, aurantiamide acetate, 5,7-dihydroxy-2-phenyl-chroman-4-one, (S)-scoulerine, pratensein, eriodictyol, ostruthin, and auraptene, probably interact with the core targets. These targets play crucial roles in a series of interconnected processes closely associated with bacterial infection. For instance, AKT1 is responsible for regulating *S. aureus* infection, and the inhibition of glyceraldehyde-3-phosphate dehydrogenase (GAPDH) activity contributed to the attenuation of bacterial growth (Gómez *et al*., 2019; Xu *et al*., 2013). Moreover, hypoxia inducible factor 1 (HIF1A) has been recognized for its significant role in the immune response by enhancing autophagy to fight infections caused by various pathogens (Neubert *et al*., 2019). Studies have indicated that tumor necrosis factor (TNF) and epidermal growth factor receptor (EGFR) are critical components of both the antibacterial protective and the inflammatory responses to infections (Chitturi *et al*., 2022; Liu *et al*., 2024). Additionally, Matrix metalloproteinase 2 (MMP2) and MMP9 play critical roles in regulating infectious inflammation in response to pathogen-associated molecular patterns. They contribute to extracellular matrix (ECM) remodeling, immune cell recruitment, and cytokine activation, which are essential for host defense but can also exacerbate tissue damage if dysregulated

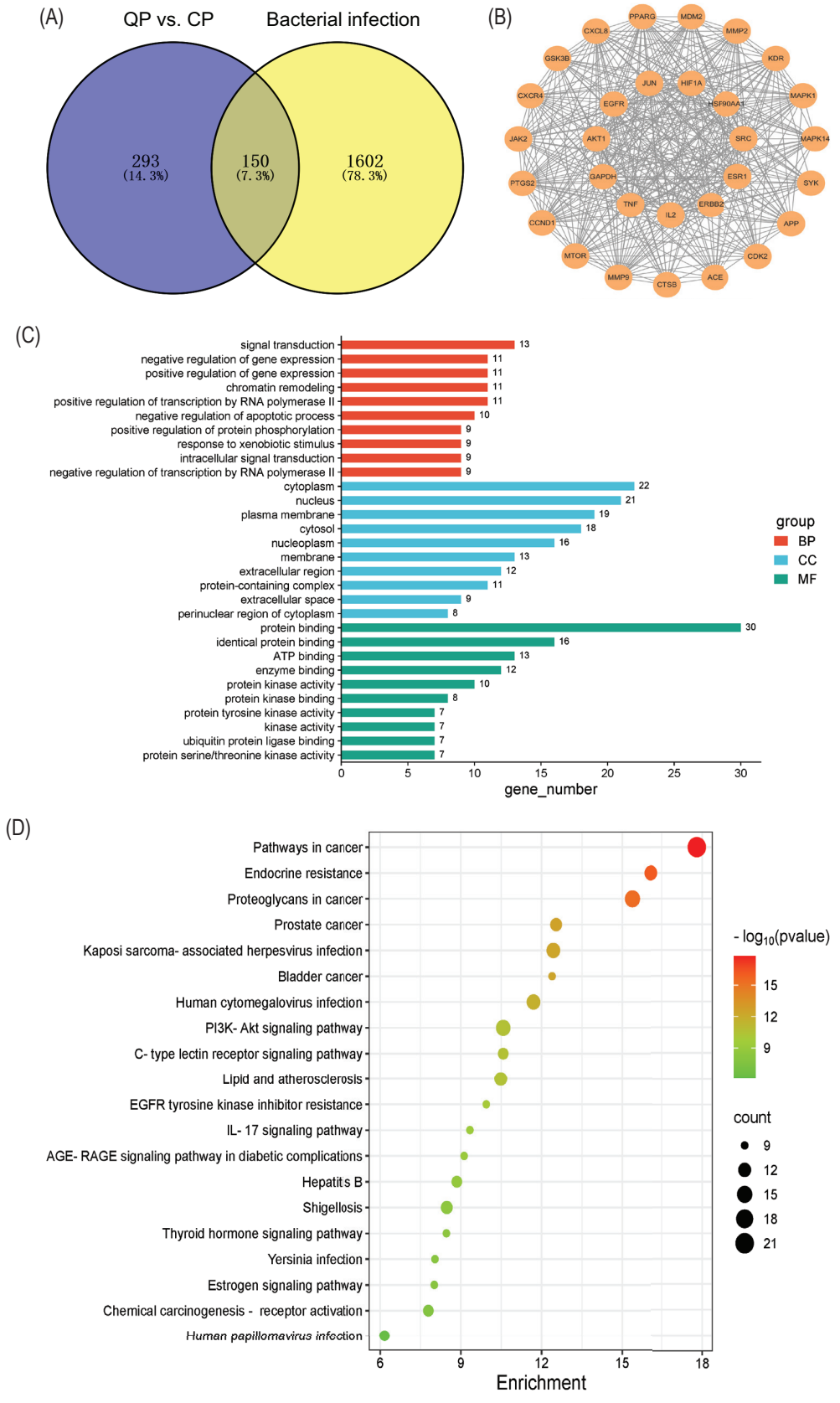

Figure 4. The network of metabolites–targets–bacterial infection in the QP vs CP comparison group. (A) Venn diagram illustrating the overlapping targets between the potential active components of the QP vs CP group and bacterial infection. (B) Core target network of antibacterial targets of the potential active components in QP, comprising 30 nodes and 383 edges. (C) The top 10 functional terms from GO enrichment analysis based on the core targets of QP. (D) The top 20 pathways from KEGG pathway enrichment analysis based on the core targets of QP.

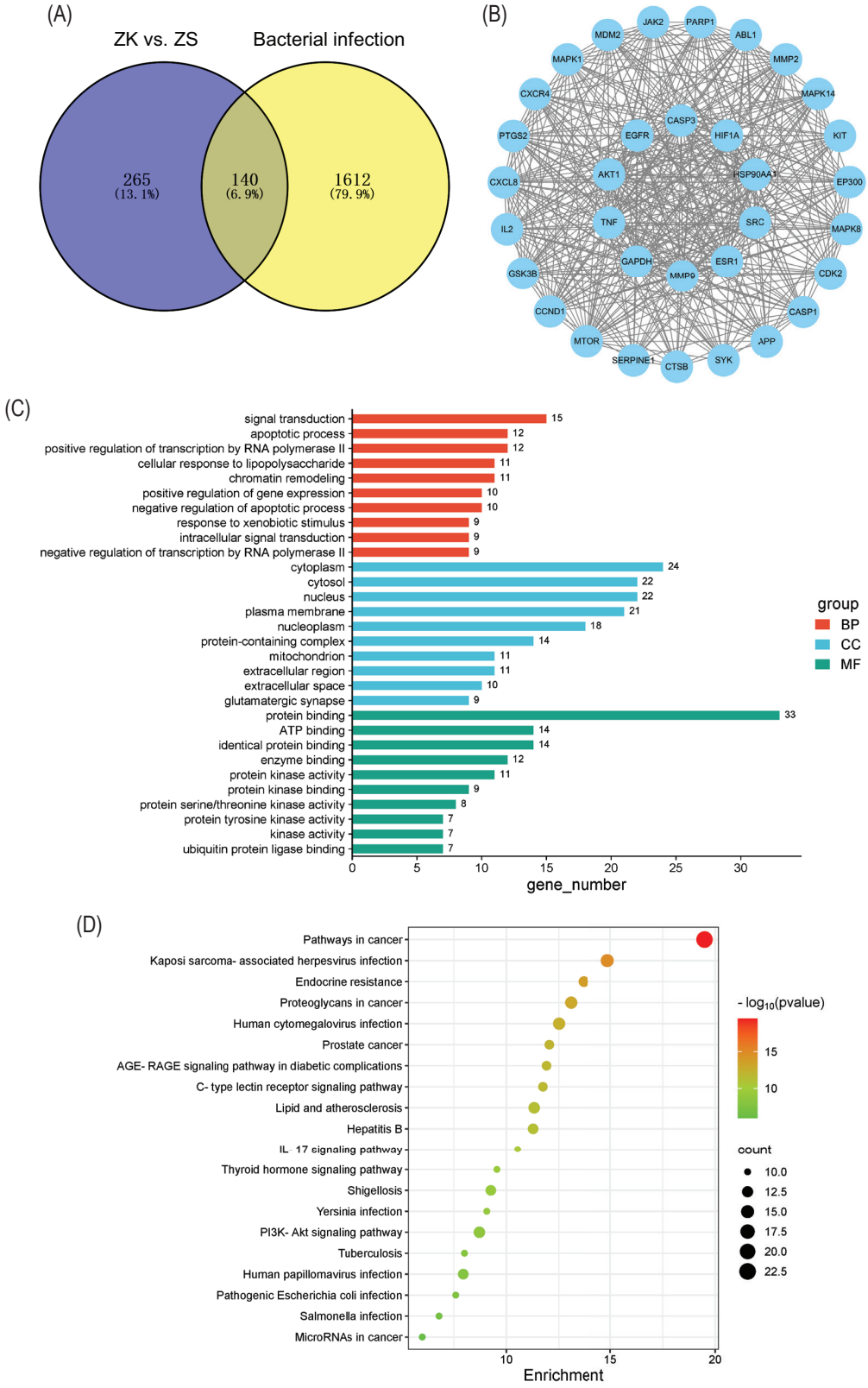

Figure 5. The network of metabolites–targets–bacterial infection in the ZK vs ZS comparison group. (A) Venn diagram illustrating the overlapping targets between the potential active components of the ZK vs ZS group and bacterial infection. (B) Core target network of antibacterial targets of the potential active components in ZK, containing 33 nodes and 438 edges. (C) The top 10 functional terms from GO enrichment analysis based on the core targets of ZK. (D) The top 20 pathways from KEGG pathway enrichment analysis based on the core targets of ZK.

(García-López *et al*., 2023). Emerging evidence identifies glycogen synthase kinase 3β (GSK3β) as a central regulator of innate immune responses to bacterial challenges. During bacterial infections, GSK3β activity influences phagocytic functions of macrophages and neutrophils, as well as the balance between pro- and anti-inflammatory responses (Cortés-Vieyra *et al*., 2021). These findings provide valuable insights into the potential antibacterial targets of QP and ZK, underscoring their therapeutic potential in combating bacterial infections.

To further reveal the mechanisms underlying the significant antibacterial activity of QP and ZK extracts, we conducted GO functional and KEGG pathway enrichment analyses on the core target genes using the DAVID bioinformatics tool. The top 10 biological processes (BPs), cellular components (CCs), and molecular functions (MFs) associated with QP and ZK extracts are presented in Figures 4C and 5C, respectively. The potential active components of QP extracts were implicated in BPs, including signal transduction, gene expression, and positive regulation of transcription by RNA polymerase II. Regarding CCs, the notable entries included cytoplasm, nucleus, and plasma membrane. In terms of MFs, the enriched terms mainly involved protein binding, ATP binding, enzyme binding, and protein kinase activity. In addition, our analysis identified KEGG signaling pathways associated with the antibacterial activity of QP and ZK extracts, with the top 20 pathways displayed in Figures 4D and 5D, respectively. Notably, the bacterial infection-related targets of QP and ZK extracts were linked to "pathway in cancer," "endocrine resistance," and "Kaposi sarcoma-associated herpesvirus infection." Extensive research has elucidated the pivotal contribution of endocrine resistance pathways to breast cancer progression (Dimitrakopoulos *et al*., 2021). We hypothesize that the molecular mechanisms underlying endocrine resistance in cancer, such as AKT1/MAPK signaling, efflux pump activation, and biofilm formation, may influence bacterial survival. This mechanistic overlap suggests a promising cross-disciplinary approach in which endocrine pathway modulators could be repurposed as antibacterial adjuvants. Bacterial infections (e.g., *Staphylococcus*, *Pseudomonas*) are common in immunosuppressed Kaposi sarcoma-associated herpesvirus (KSHV) infection patients, exacerbating inflammation and viral reactivation (Angius *et al*., 2017; Markazi *et al*., 2021). QP and ZK extracts may target bacterial virulence factors that synergize with KSHV oncoproteins. These results indicate that the potential antibacterial compounds in citrus herbs exert their effects by interacting with the cancer-related and infection resistance-related pathways.

Molecular docking validation of potential active components and core targets

To validate the network pharmacology predictions, molecular docking was performed to evaluate the binding affinity between the key bioactive compounds and their corresponding core target proteins. Binding energy values reflect the likelihood of receptor–ligand interaction, where lower energy indicates higher affinity and greater complex stability (Noor *et al*., 2022). Among the tested interactions, linarin showed the lowest binding affinity with TNF (−10.22 kcal/mol), while limonin exhibited a similarly strong binding to GSK3B (−10.22 kcal/mol). The molecular docking results are visualized in Figures 6A and 6B. Structurally, linarin formed hydrogen bonds with Lys98, Ser99, Tyr115, and Gln102 (one bond each), and two hydrogen bonds with Arg103 in TNF (Figure 6A). In GSK3B, linarin interacted with Gln185 and Tyr140, each through a single hydrogen bond (Figure 6B). Previous studies have demonstrated that linarin exhibits potent inhibitory effects against *Chlamydia pneumoniae* even at low concentrations (Mottaghipisheh *et al*., 2021). Beyond its antibacterial properties, linarin has also been found

(A)

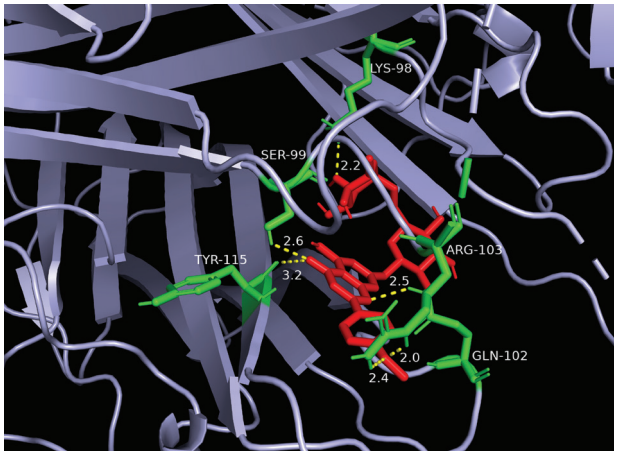

(B)

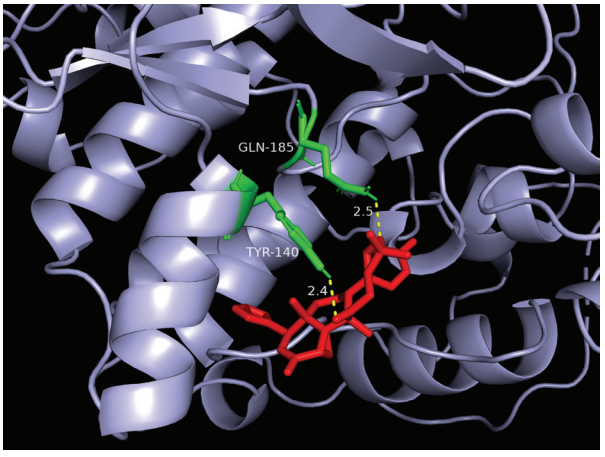

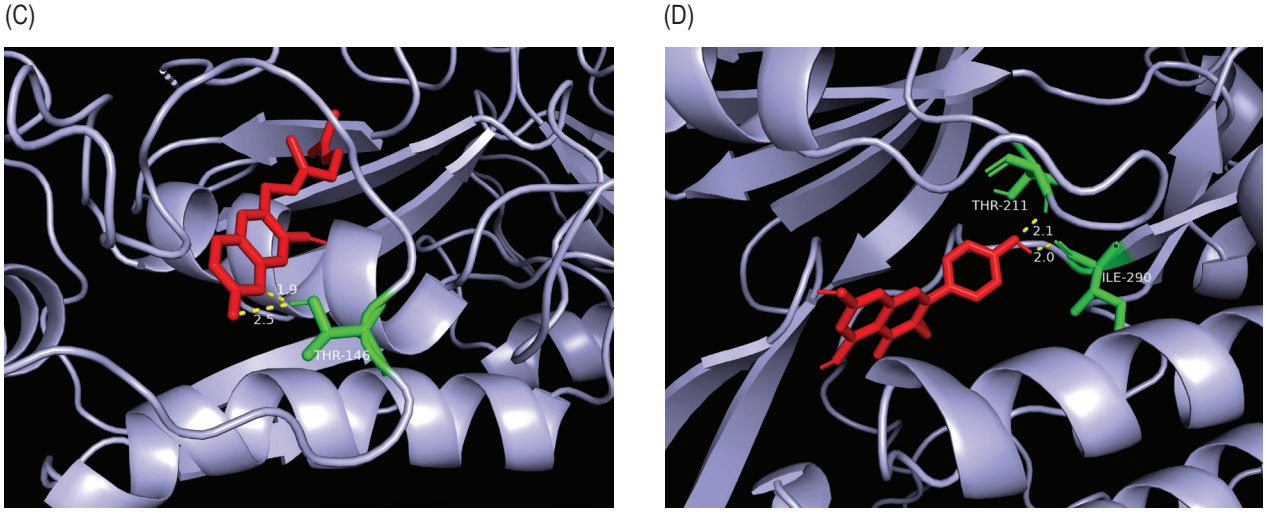

Figure 6. The docking model of linarin with TNF (A) and GSK3B (B); ostruthin with MMP2 (C); kaempferol 3-methyl ether with AKT1 (D). Active site residues are in green-colored lines. Hydrogen bonds formed between protein and compound are shown as yellow dotted lines.

to suppress key proinflammatory cytokines, such as TNF-α, IL-1β, and IL-6, effectively mitigating renal inflammation (Qian *et al*., 2025). Building on this evidence, our findings suggest that linarin may interact with key targets identified in this study, highlighting its potential as a novel therapeutic strategy against bacterial infections. Additionally, ostruthin showed antibacterial activity against both *S. aureus* and MRSA, with MIC values of 12.5 and 25 μM, respectively (Zwirchmayr *et al*., 2023). Ostruthin displayed strong binding to MMP2 (−9.92 kcal/mol), forming two hydrogen bonds with Thr146 (Figure 6C). Meanwhile, the small molecule kaempferol 3-methyl ether showed a compact binding pattern with the AKT1 protein active pocket with low binding affinity (−9.31 kcal/mol), stabilizing the complex via hydrogen bonds with Thr211 and Ile290 (Figure 6D). AKT1 is a significant regulator of cellular signaling pathways, regulating cell growth, metabolism, and survival, which positions it as a promising therapeutic target for inflammatory and cancer-related diseases (Duggal *et al*., 2018). Emerging evidence suggests that AKT1-mediated signaling may also influence host–pathogen interactions, potentially modulating immune responses during bacterial infections. This dual role in both disease pathogenesis and host defense establishes AKT1 as a potential target for therapeutic intervention in infectious diseases.

Conclusion

The antibacterial activity of citrus herb extracts QP, CP, ZK, and ZS was evaluated, indicating that QP and ZK extracts exhibited stronger potency against both *B. cereus* and MRSA compared to CP and ZS. Multivariate analysis showed the significant metabolite variations between the QP and CP comparison groups, as well as between the ZK and ZS comparison groups. Metabolomics profiling of citrus herb extracts, combined with network pharmacology, was employed to identify the potential active components and their targets, highlighting key targets, such as TNF, GAPDH, and AKT1. The molecular docking results showed that potential active components, such as skimmin, linarin, ostruthin, kaempferol 3-methyl ether, and limonin, spontaneously bound to core target proteins. Therefore, this study identifies antibacterial components in citrus herbs and proposes a potential mechanism for preventing bacterial infections, suggesting their potential as natural preservatives in food safety or complementary agents against antibiotic-resistant bacteria. However, there are some limitations in this study. The network pharmacology analysis relied on existing databases, which may not comprehensively cover all potential target genes and pathways related to bacterial infections. A more extensive and up-to-date database would improve the reliability and accuracy of our predictions. Although we combined network pharmacology with molecular docking, these approaches could not fully elucidate the precise molecular interactions or dynamic biological processes underlying the therapeutic mechanisms of ZK and QP against bacterial infections. Furthermore, experimental validation using animal models or cell-based assays would strengthen our findings. For example, *in vitro* antibacterial assays could be conducted to confirm the efficacy of the core components against *B. cereus* and MRSA, and cell-based assays utilizing Western blotting and qPCR could be employed to validate the modulation of the key targets and pathways.

Acknowledgments

This work was supported by Zhaoqing University Youth Program (Grant No. QN202446 and QN202450), Zhaoqing City Science and Technology Innovation Guidance Project (No. 241218104169431), and Innovative Research Team Funding Project of Zhaoqing University (Grant No. TD202414).

Authors Contributions

Y. Li conducted the experiments, analyzed the data, and wrote the manuscript. L. He performed the experiments, contributed to the graph visualization, and modified the manuscript. Y. Liang helped with experiments and did the validation. All authors have read and agreed to the submitted version of the manuscript.

Conflicts of Interest

The authors declare that there are no conflicts of interest.

References

Adusei, S., Otchere, J.K., Oteng, P., Mensah, R.Q. and Tei-Mensah, E., 2019. Phytochemical analysis, antioxidant and metal chelating capacity of *Tetrapleura tetraptera*. Heliyon 5(11): e02762. https://doi.org/10.1016/j.heliyon.2019.e02762

Agu, P.C., Afiukwa, C.A., Orji, O.U., Ezeh, E.M., Ofoke, I.H., Ogbu, C.O., et al., 2023. Molecular docking as a tool for the discovery of molecular targets of nutraceuticals in diseases management. Scientific Reports 13(1): 13398. https://doi.org/10.1038/s41598-023-40160-2

Akhter, S., Arman, M.S.I., Tayab, M.A., Islam, M.N. and Xiao, J., 2024. Recent advances in the biosynthesis, bioavailability, toxicology, pharmacology, and controlled release of citrus neohesperidin. Critical Reviews in Food Science and Nutrition 64(15): 5073–5092. https://doi.org/10.1080/10408398.2022.2149466

Angius, F., Piras, E., Uda, S., Madeddu, C., Serpe, R., Bigi, R., et al., 2017. Antimicrobial sulfonamides clear latent Kaposi sarcoma herpesvirus infection and impair MDM2–p53 complex formation. The Journal of Antibiotics 70(9): 962–966. https://doi.org/10.1038/ja.2017.67

Bai, J., Wu, Y., Bu, Q., Zhong, K. and Gao, H., 2022. Comparative study on antibacterial mechanism of shikimic acid and quinic acid against *Staphylococcus aureus* through transcriptomic and metabolomic approaches. LWT 153: 112441. https://doi.org/10.1016/j.lwt.2021.112441

Cao, X., Shi, K., Xu, Y., Zhang, P., Zhang, H. and Pan, S., 2023. Integrated metabolomics and network pharmacology to reveal antioxidant mechanisms and potential pharmacological ingredients of citrus herbs. Food Research International 174: 113514. https://doi.org/10.1016/j.foodres.2023.113514

Cebi, N. and Erarslan, A., 2023. Determination of the antifungal, antibacterial activity and volatile compound composition of citrus bergamia peel essential oil. Foods 12(1): 203. https://doi.org/10.3390/foods12010203

Chen, L., Zhao, N., Cao, J., Liu, X., Xu, J., Ma, Y., et al., 2022. Short- and long-read metagenomics expand individualized structural variations in gut microbiomes. Nature Communications 13: 3175. https://doi.org/10.1038/s41467-022-30857-9

Chen, Y., Pan, H., Hao, S., Pan, D., Wang, G. and Yu, W., 2021. Evaluation of phenolic composition and antioxidant properties of different varieties of Chinese citrus. Food Chemistry 364: 130413. https://doi.org/10.1016/j.foodchem.2021.130413

Chitturi, K.R., Burns, E.A., Muhsen, I.N., Anand, K. and Trachtenberg, B.H., 2022. Cardiovascular risks with epidermal growth factor receptor (EGFR) tyrosine kinase inhibitors and monoclonal antibody therapy. Current Oncology Reports 24(4): 475–491. https://doi.org/10.1007/s11912-022-01215-1

Ciriminna, R., Petri, G.L., Angellotti, G., Luque, R., Fabiano Tixier, A.S., Meneguzzo, F., et al., 2025. Citrus flavonoids as antimicrobials. Chemistry & Biodiversity 22(6): e202403210. https://doi.org/10.1002/cbdv.202403210

Cortés-Vieyra, R., Silva-García, O., Gómez-García, A., Gutiérrez-Castellanos, S., Álvarez-Aguilar, C., & Baizabal-Aguirre, V. M. (2021). Glycogen synthase kinase 3β modulates the inflammatory response activated by bacteria, viruses, and parasites. Frontiers in Immunology 12: 675751. https://doi.org/10.3389/fimmu.2021.675751

Costa, J.H., Bazioli, J.M., de Moraes Pontes, J.G. and Fill, T.P., 2019. *Penicillium digitatum* infection mechanisms in citrus: What do we know so far? Fungal Biology 123(8): 584–593. https://doi.org/10.1016/j.funbio.2019.05.004

D'Amore, T., Chaari, M., Falco, G., De Gregorio, G., Zaraî Jaouadi, N., Ali, D.S., et al., 2024. When sustainability meets health and innovation: The case of Citrus by-products for cancer chemoprevention and applications in functional foods. Biocatalysis and Agricultural Biotechnology 58: 103163. https://doi.org/https://doi.org/10.1016/j.bcab.2024.103163

Dimitrakopoulos, F.-I., Kottorou, A. and Tzezou, A., 2021. Endocrine resistance and epigenetic reprogramming in estrogen receptor positive breast cancer. Cancer Letters 517: 55–65. https://doi.org/https://doi.org/10.1016/j.canlet.2021.05.030

Duggal, S., Jailkhani, N., Midha, M.K., Agrawal, N., Rao, K.V.S. and Kumar, A., 2018. Defining the Akt1 interactome and its role in regulating the cell cycle. Scientific Reports 8(1),\: 1303. https://doi.org/10.1038/s41598-018-19689-0

Ellouze, I., Ben Akacha, B., Mekinić, I.G., Ben Saad, R., Kačániová, M., Kluz, M.I., et al., 2024. Enhancing antibacterial efficacy: Synergistic effects of *Citrus aurantium* essential oil mixtures against *Escherichia coli* for food preservation. Foods 13(19): 3093. https://doi.org/10.3390/foods13193093

Gao, Z., Gao, W., Zeng, S.-L., Li, P. and Liu, E.H., 2018. Chemical structures, bioactivities and molecular mechanisms of citrus polymethoxyflavones. Journal of Functional Foods 40: 498–509. https://doi.org/10.1016/j.jff.2017.11.036

García-López, C., Rodríguez-Calvo-de-Mora, M., Borroni, D., Sánchez-González, J.-M., Romano, V. and Rocha-de-Lossada, C.,

2023. The role of matrix metalloproteinases in infectious corneal ulcers. Survey of Ophthalmolog 68(5): 929–939. https://doi.org/10.1016/j.survophthal.2023.06.007

Gómez, S., Querol-García, J., Sánchez-Barrón, G., Subias, M., González-Alsina, À., Franco-Hidalgo, V., et al., 2019. The antimicrobials anacardic acid and curcumin are not-competitive inhibitors of gram-positive bacterial pathogenic glyceraldehyde-3-phosphate dehydrogenase by a mechanism unrelated to human C5a anaphylatoxin binding. Frontiers in Microbiology 10: 326. https://doi.org/10.3389/fmicb.2019.00326

Guo, H., Chen, Y.-H., Wang, T.-M., Kang, T.-G., Sun, H.-Y., Pei, W.-H., et al., 2021. A strategy to discover selective α-glucosidase/acetylcholinesterase inhibitors from five function-similar citrus herbs through LC-Q-TOF-MS, bioassay and virtual screening. Journal of Chromatography B 1174: 122722. https://doi.org/10.1016/j.jchromb.2021.122722

Hao, X.-T., Peng, R., Guan, M., Zhang, H.-J., Guo, Y., Shalapy, N.M., et al., 2024. The food and medicinal homological resources benefiting patients with hyperlipidemia: categories, functional components, and mechanisms. Food & Medicine Homology 1(2): 9420003. https://doi.org/10.26599/fmh.2024.9420003

Impey, R.E., Hawkins, D.A., Sutton, J.M. and Soares da Costa, T.P., 2020. Overcoming intrinsic and acquired resistance mechanisms associated with the cell wall of Gram-negative bacteria. Antibiotics 9(9): 623. https://doi.org/10.3390/antibiotics9090623

Li, Y., Dalabasmaz, S., Gensberger-Reigl, S., Heymich, M.-L., Krofta, K. and Pischetsrieder, M., 2023. Identification of colupulone and lupulone as the main contributors to the antibacterial activity of hop extracts using activity-guided fractionation and metabolome analysis. Food Research International 169: 112832. https://doi.org/10.1016/j.foodres.2023.112832

Liu, H., Lin, J., Phan, Q.T., Bruno, V.M. and Filler, S.G., 2024. Epidermal growth factor receptor signaling governs the host inflammatory response to invasive aspergillosis. mBio 15: e0267124. https://doi.org/10.1128/mbio.02671-24

Liu, J., Liu, J., Tong, X., Peng, W., Wei, S., Sun, T., et al., 2021. Network pharmacology prediction and molecular docking-based strategy to discover the potential pharmacological mechanism of Huai Hua San against ulcerative colitis. Drug Design, Development and Therapy 15: 3255–3276. https://doi.org/10.2147/dddt.S319786

Liu, N., Li, X., Zhao, P., Zhang, X., Qiao, O., Huang, L., et al., 2021. A review of chemical constituents and health-promoting effects of citrus peels. Food Chemistry 365: 130585. https://doi.org/10.1016/j.foodchem.2021.130585

Liu, Z., Pan, Y., Li, X., Jie, J. and Zeng, M., 2017. Chemical composition, antimicrobial and anti-quorum sensing activities of pummelo peel flavonoid extract. Industrial Crops and Products 109: 862–868. https://doi.org/10.1016/j.indcrop.2017.09.054

Ma, A., Zou, F., Zhang, R. and Zhao, X., 2022. The effects and underlying mechanisms of medicine and food homologous flowers on the prevention and treatment of related diseases. Journal of Food Biochemistry 46(12): e14430. https://doi.org/https://doi.org/10.1111/jfbc.14430

Mannucci, C., Calapai, F., Cardia, L., Inferrera, G., D'Arena, G., Di Pietro, M., et al., 2018. Clinical pharmacology of *Citrus aurantium* and *Citrus sinensis* for the treatment of anxiety. Evidence-Based Complementary and Alternative Medicine 3624094: 1–18. https://doi.org/10.1155/2018/3624094

Maqbool, Z., Khalid, W., Atiq, H.T., Koraqi, H., Javaid, Z., Alhag, S.K., et al., 2023. Citrus waste as source of bioactive compounds: Extraction and utilization in health and food industry. Molecules 28(4): 1636. https://doi.org/10.3390/molecules28041636

Markazi, A., Meng, W., Bracci, P.M., McGrath, M.S. and Gao, S.-J., 2021. The role of bacteria in KSHV infection and KSHV-induced cancers. Cancers 13(17): 4269. https://doi.org/10.3390/cancers13174269

Mottaghipisheh, J., Taghrir, H., Boveiri Dehsheikh, A., Zomorodian, K., Irajie, C., Mahmoodi Sourestani, M., et al., 2021. Linarin, a glycosylated flavonoid, with potential therapeutic attributes: A comprehensive review. Pharmaceuticals 14(11): 1104. https://doi.org/10.3390/ph14111104

Neubert, P., Weichselbaum, A., Reitinger, C., Schatz, V., Schröder, A., Ferdinand, J. R., et al., 2019. HIF1A and NFAT5 coordinate Na+-boosted antibacterial defense via enhanced autophagy and autolysosomal targeting. Autophagy 15(11): 1899–1916. https://doi.org/10.1080/15548627.2019.1596483

Ni, J., Guo, Y., Chang, N., Cheng, D., Yan, M., Jiang, M., et al., 2019. Effect of *N*-methyltyramine on the regulation of adrenergic receptors via enzymatic epinephrine synthesis for the treatment of gastrointestinal disorders. Biomedicine & Pharmacotherapy 111: 1393–1398. https://doi.org/10.1016/j.biopha.2018.12.145

Noor, F., Rehman, A., Ashfaq, U.A., Saleem, M.H., Okla, M.K., Al-Hashimi, A., et al., 2022. Integrating network pharmacology and molecular docking approaches to decipher the multi-target pharmacological mechanism of *Abrus precatorius* L. acting on diabetes. Pharmaceuticals 15(4): 414. https://doi.org/10.3390/ph15040414

Qian, Y., Zhang, Y., Chen, Y., Wang, X., Liu, L., Yu, H., et al., 2025. Linarin attenuates hyperuricemic nephropathy by modulating Nrf2/Keap1 and TLR4/NF-κB signaling pathways. Phytomedicine 139: 156440. https://doi.org/10.1016/j.phymed.2025.156440

Shady, N.H., Mokhtar, F.A., Mahmoud, B.K., Yahia, R., Ibrahim, A.M., Sayed, N.A., et al., 2024. Capturing the antimicrobial profile of Paeonia officinalis, Jasminum officinale and Rosa damascene against methicillin resistant *Staphylococcus aureus* with metabolomics analysis and network pharmacology. Scientific Reports 14: 13621. https://doi.org/10.1038/s41598-024-62369-5

Shraim, A.M., Ahmed, T.A., Rahman, M.M. and Hijji, Y.M., 2021. Determination of total flavonoid content by aluminum chloride assay: A critical evaluation. LWT 150: 111932. https://doi.org/10.1016/j.lwt.2021.111932

Tang, W., Zhang, Z., Nie, D., Liu, S., Li, Y., Liu, M., et al., 2023. Selective antibacterial activity of *Citrus Medica limonum* essential oil against *Escherichia coli* K99 and *Lactobacillus acidophilus* and its antibacterial mechanism. LWT 186: 115215. https://doi.org/10.1016/j.lwt.2023.115215

Tian, F., He, X.F., Sun, J., Liu, X.D., Zhang, Y., Cao, H., et al., 2019. Simultaneous quantitative analysis of nine constituents in six Chinese medicinal materials from Citrus genus by high-performance liquid chromatography and high-resolution mass

spectrometry combined with chemometric methods. Journal of Separation Science 43(4): 736–747. https://doi.org/10.1002/jssc.201901033

Wang, W., Xu, L., Zhang, Y., Cao, Y., Yang, Y., Liu, G., et al., 2025. Effects of Chenpi (*Citrus reticulata* cv. *Chachiensis*) on serum antioxidant enzymes, inflammatory factors, and intestinal health in Beagle dogs. Frontiers in Microbiology 15: 1415860. https://doi.org/10.3389/fmicb.2024.1415860

Xu, F., Kang, Y., Zhang, H., Piao, Z., Yin, H., Diao, R., et al., 2013. Akt1-mediated regulation of macrophage polarization in a murine model of *Staphylococcus aureus* pulmonary infection. The Journal of Infectious Diseases 208(3): 528–538. https://doi.org/10.1093/infdis/jit177

Yu, X., Sun, S., Guo, Y., Liu, Y., Yang, D., Li, G., et al., 2018. Citri Reticulatae Pericarpium (Chenpi): Botany, ethnopharmacology, phytochemistry, and pharmacology of a frequently used traditional Chinese medicine. Journal of Ethnopharmacology 220: 265–282. https://doi.org/10.1016/j.jep.2018.03.031

Zhang, W., Liu, D., Fu, X., Xiong, C. and Nie, Q., 2022. Peel essential oil composition and antibacterial activities of *Citrus x sinensis* L. Osbeck "Tarocco" and *Citrus reticulata* Blanco. Horticulturae 8: 793. https://doi.org/10.3390/horticulturae8090793

Zhao, C., Wang, F., Lian, Y., Xiao, H. and Zheng, J., 2018. Biosynthesis of citrus flavonoids and their health effects. Critical Reviews in Food Science and Nutrition 60(4): 566–583. https://doi.org/10.1080/10408398.2018.1544885

Zhao, S., Liu, Z., Wang, M., He, D., Liu, L., Shu, Y., et al., 2018. Anti-inflammatory effects of Zhishi and Zhiqiao revealed by network pharmacology integrated with molecular mechanism and metabolomics studies. Phytomedicine 50: 61–72. https://doi.org/10.1016/j.phymed.2018.09.184

Zhou, P., Zheng, M., Li, X., Zhou, J., Shang, Y., Li, Z., et al., 2022. A consecutive extraction of pectin and hesperidin from *Citrus aurantium* L.: Process optimization, extract mechanism, characterization and bio-activity analysis. Industrial Crops and Products 182: 114849. https://doi.org/10.1016/j.indcrop.2022.114849

Zwirchmayr, J., Cruz, C.D., Grienke, U., Tammela, P. and Rollinger, J.M., 2023. Biochemometry identifies ostruthin as pluripotent antimicrobial and anthelmintic agent from masterwort. iScience 26(9):s 107523. https://doi.org/10.1016/j.isci.2023.107523